Reprinted from MONTHLY WEATHER REVIEW, Vol. 121, No. 7, July 1993
American Meteorological Society

Moist Wind Relationships

WILLIAM H. RAYMOND

Cooperative Institute for Meteorological Satellite Studies, University of Wisconsin, Madison, Wisconsin

(Manuscript received 24 July 1992, in final form 8 January 1993)

ABSTRACT

Equations describing the temporal and spatial behavior of the kinematic moisture and heat flux are introduced in this study. In these nonlinear equations, the contribution by diabatic processes to the large-scale flux is composed of two parts. One part is associated with a Rayleigh damping term, while the other arises from temporal and spatial changes in the pressure gradient term.

The influence of diabatic processes on the large-scale moisture fluxes depends greatly on the degree of balance between forcing and damping terms in the governing equations. The existence of a near balance requires a reduction in the large-scale horizontal geostrophic wind speed. From a scale analysis of the moisture flux equations it is argued that reductions in the large-scale horizontal wind speed, observed within major cumulus cloud systems, help conserve large-scale moisture fluxes. The deviation of the wind from geostrophic conditions is easily estimated. This wind modification induces secondary vertical circulations that contribute to the convergence, creating or supporting long-lived mesoscale flows. In the tropics the wind modification has an antitriptic relationship.

These diagnostic findings suggest possible modifications to the wind field in the application of cumulus parameterization, and may be important in diabatic initialization of numerical weather prediction models.

1. Introduction

In the extratropics, the large-scale atmospheric flow fluctuates about known balance conditions. Away from the major centers of cyclonic and anticyclonic activity, the horizontal wind components closely approximate geostrophy in the free atmosphere. Within strong cyclonic centers the flow is modified by curvature and by diabatic effects. To forecast the wind field in the presence of diabatic activity would require solutions of the complete equations of motion with physical processes included, which is not always practical. Otherwise, to get a snapshot of the instantaneous horizontal wind field requires solving the nonlinear diabatic balance equations. The simple wind laws, like the gradient-wind approximation, do include the effect of curvature and some indirect consequences of diabatic heating. This study outlines a simplified approach derived from first principles that identifies how diabatically induced modifications in the horizontal wind components influence the moisture and sensible heat fluxes. This study provides necessary additional information about the effect of diabatic processes on the atmospheric dynamics for use in model initialization and cumulus parameterization.

Many years of observations have shown that diabatic processes can significantly enhance cyclonic development and influence the general circulation. Many journal articles and textbooks testify to this. A small subset includes Petterssen (1956), Riehl and Malkus (1958), Kuo (1965, 1974), Yanai et al. (1973), Riehl (1979), Donner et al. (1982), Houze and Hobbs (1982), and Konig and Ruprecht (1989). Modeling studies also have verified that moist processes are important for rapid development (Kuo and Reed 1988; Reed et al. 1988). Additionally, diabatic initialization techniques are used to enhance cyclonic circulations and low-level convergence to help speed up precipitation processes in numerical forecast models (e.g., Tarbell et al. 1981; Krishnamurti et al. 1983; Krishnamurti et al. 1984; Donner 1988; Wang and Warner 1988; Turpeinen et al. 1990; Daley 1991).

There also are many studies on the effect of clouds on the large-scale dynamics, including Malkus (1952), Schneider and Lindzen (1976), Sui and Yanai (1986), Cho (1985), and Konig and Ruprecht (1989). The vertical transport of atmospheric properties in clouds is important because the cloud vertical velocity is much larger than that found in the environment, especially in the tropics. In contrast, the magnitudes of the horizontal flow in the cloud and environment are of the same order, but according to the above studies, mixing, vertical transport, and other processes are responsible for some deceleration of the mean flow by "cumulus friction" (Malkus 1952; Schneider and Lindzen 1976). Several articles propose parameterizations of cumulus convection effects on the large-scale vorticity or momentum. Approaches include mass entrainment and

Corresponding author address: Dr. William H. Raymond, CIMMS/University of Wisconsin, 1225 West Dayton St., Madison, WI 53706.

detrainment concepts (Ooyama 1971), vertical transport and properties from simple cloud models (Shapiro and Stevens 1980), the introduction of drag terms (Esbensen et al. 1987; Austin and Houze 1973), and other representations of cumulus friction (Schneider and Lindzen 1976). In this study a different method is proposed to estimate the cumulus friction process.

Gill (1980) has examined tropical circulation forced by localized heating, while Heckley and Gill (1984) have studied transient features in the tropics when the heating is impulsively started. In these studies the role of diabatic heating on the large-scale flow is modeled by adding a forcing term to the continuity equation in the linearized shallow-water model. The forcing modifies the pressure and its gradients, which in turn modify the horizontal wind field. This model is conceptually simple yet captures the essence of the large-scale response to diabatic forcing arising from thermal changes. Gill (1980) heuristically added a Rayleigh damping term with constant coefficient over the entire domain of his linear model, which produced a steady state, but this was not intended to represent the cumulus friction process, and it provided no insight on why cumulus friction occurs, its region of influence, or consequences. Holton and Colton (1972) in their linear vorticity model also found that damping was needed to obtain agreement with observations.

Lorenz (1978) has identified some optimal atmospheric energetic arrangements, but local optimal relationships remain unknown if they exist at all. One can speculate that cumulus friction is partially an atmospheric response for conserving basic large-scale atmospheric properties or optimizing fundamental parameters like the kinetic energy, enthalpy, etc. Clearly, temporal and advective changes in moisture flux, heat flux, and entropy are influenced by cumulus friction.

In this diagnostic study it is found that mesoscale moist processes introduce into the moisture and heat flux equations a Rayleigh damping term that depends upon the condensation and evaporation rate. This friction allows changes in the large-scale moisture fluxes to remain relatively small provided a near balance exists between the forcing and damping terms. Scale analysis shows that this balance involves the pressure gradient, Coriolis, and Rayleigh damping term. Balance further requires a reduction in the large-scale horizontal geostrophic wind speed, that is, the creation of an ageostrophic wind. Clearly, if the horizontal wind is reduced excessively, then the balance condition breaks down. Our hypothesis is that for long-lived mesoscale convection the large-scale horizontal winds do not differ greatly from that needed to establish a near balance between the pressure gradient, Coriolis, and Rayleigh damping terms. It is found diagnostically and in numerical applications that the ageostrophic wind enhances the existing convergence and establishes a mesoscale vertical circulation within the large-scale flow to help balance the modified horizontal wind.

To illustrate our hypothesis we examine the behavior of the kinematic moisture and heat flux. The derivation of these equations is quite simple, but they yield surprising information. In these equations the contribution of diabatic heating to the horizontal wind components is naturally partitioned into two parts. One diabatic contribution is contained within the geostrophic wind component (pressure gradient term), while the remaining one is associated with the Rayleigh damping (condensation) or forcing (evaporation) term. To examine the importance of the terms in the flux component equations, a scale analysis is preformed and simplified solutions are found. For nontropical regions our approximate solutions are given in terms of the geostrophic flow. In some of our illustrative examples a time scale less than the inverse of the Coriolis parameter is required; however, the flux equations are valid even when this is not true. In tropical regions any tendency toward moisture flux conservation enhances the relationship between the pressure gradient term and the Rayleigh damping term. This induces secondary antitriptic circulations. A simple hurricane model is presented to illustrate the wind modifications associated with any enhancement toward moisture flux conservation. Also tested are applications in cumulus parameterization.

2. The equations

The inviscid equations (Haltiner and Williams 1980, pp. 16, 17, and 308) for large-scale flow describing horizontal wind components u and v, the temperature T, potential temperature θ, the mixing ratio q, and pressure p are

$$\frac{du}{dt} = -\frac{1}{\rho}\frac{\partial p}{\partial x} + fv, \tag{1}$$

$$\frac{dv}{dt} = -\frac{1}{\rho}\frac{\partial p}{\partial y} - fu, \tag{2}$$

$$\frac{d\theta}{dt} = -\frac{L\theta Q}{Tc_p}, \tag{3}$$

$$\frac{dq}{dt} = Q. \tag{4}$$

The total derivative $d(\ )/dt$, x, y, z, and t have the standard definitions. The Coriolis parameter f satisfies $f = 2\Omega \sin\phi$, where Ω is the angular velocity of the earth and ϕ is the latitude. Here ρ is the density, g is the acceleration due to gravity, c_p is the specific heat for constant pressure, L is the latent heat of condensation or evaporation, and Q is the condensation or evaporation rate. Here Q is a sink for condensation and a source for evaporation and sublimation from saturated air; otherwise, $Q = 0$ when q is below saturation. This is expressed formally by

$$Q = \frac{dq_s}{dt}. \tag{5}$$

Evaporation from the earth's surface is not explicitly included in the foregoing inviscid model. Adding the continuity equation to the four preceding equations enables the vertical motion to also be computed. For large-scale flow the hydrostatic and ideal gas laws complete the list of equations.

The transfer of moisture or heat per unit area per unit time represents the moisture or heat flux. The kinematic flux form is consistent with atmospheric measurements of temperature, mixing ratio, and wind speed and direction (Stull 1988). For example, the kinematic moisture flux has components qu, qv, and qw, while the same quantities for the kinematic sensible heat flux are θu, θv, and θw. To find the component equations governing the temporal and spatial distribution of the horizontal kinematic moisture flux, multiply (1) and (2) by the mixing ratio q and rearrange by application of the chain rule and (4). (A similar process involving the potential temperature yields the kinematic heat flux equations described in the Appendix.) The equations for the horizontal components of the total moisture flux are

$$\frac{d(qu)}{dt} = -\frac{q}{\rho}\frac{\partial p}{\partial x} + qfv + Aqu, \tag{6}$$

$$\frac{d(qv)}{dt} = -\frac{q}{\rho}\frac{\partial p}{\partial y} - qfu + Aqv. \tag{7}$$

Along with the total derivative, note that each nonlinear flux component equation contains a pressure gradient term, a term containing the Coriolis parameter, and a term that includes the factor $A = Q/q$. The A coefficient[1] is negative for condensation, making Aqu and Aqv Rayleigh damping terms. Thus, regardless of the sign of qu and qv, the damping term always reduces the magnitude of the flux. In contrast, evaporation induces a forcing response that enhances the magnitude of the flux. In tropical regions the term containing the Coriolis parameter f is small and may be ignored without introducing large errors. Then, changes to the kinematic flux depend on the residual of the pressure gradient and damping terms.

Away from the tropics the pressure gradient can be expressed in terms of the large-scale geostrophic wind

$$v_g \equiv \frac{1}{f\rho}\frac{\partial p}{\partial x}, \tag{8}$$

$$u_g \equiv \frac{-1}{f\rho}\frac{\partial p}{\partial y}. \tag{9}$$

It should be noted that diabatic contributions to the pressure field are implicitly included in the definition of the geostrophic wind. In addition, the Rayleigh damping term is important, while other indirect and feedback diabatic influences on the large-scale flow occur, but are not considered in this study. Using the geostrophic approximation simplifies (6) and (7), yielding

$$\frac{d(qu)}{dt} = -qf(v_g - v) + Aqu, \tag{10}$$

$$\frac{d(qv)}{dt} = qf(u_g - u) + Aqv. \tag{11}$$

The moisture flux is conservative in (10) and (11) for adiabatic and frictionless conditions, and for geostrophic flow. If the wind components were to remain geostrophic during a condensation event, then significant reductions in the kinematic moisture flux would occur because of the cumulative effects of the Rayleigh damping. The exact nature of any optimal *local* response in the moisture flux, heat flux, energy, or other basic atmospheric state is unknown. Scale analysis (given below), however, suggests that the large-scale moisture flux is nearly conserved. Even though the surface evaporation process slowly builds up the atmospheric water vapor, condensation can quickly deplete local supplies unless there exists a mesoscale circulation to help replenish the local reservoir. Any hypotheses that say there is a tendency toward conservation of moisture flux must also include some mechanism for generating vertical circulations.

One way to make the left-hand sides of (10) and (11) small in magnitude is to alter the wind components u and v so that the right-hand sides are closer to being balanced but not necessarily identically balanced. It is our hypothesis that the reduction in the large-scale horizontal wind components observed during major long-lived precipitating events help preserve the large-scale moisture flux. This reduction in velocity speed decreases the change in the synoptic-scale kinematic moisture flux that would otherwise occur if the wind speed remained unchanged. As will be shown in the example and applications in sections 3 and 4, this modification also enhances the longevity of the disturbance and minimizes loss in the moisture flux by creating a mesoscale vertical circulation that helps restore or pump additional moisture into the storm. Much of the discussion that follows examines the nature of the changes in the large-scale horizontal wind components that are needed to support our hypothesis.

A scale analysis of (1) and (2) shows that for large-scale conditions the pressure gradient and Coriolis force terms are larger in magnitude than the contribution from the total derivative (Holton 1979). In a similar

[1] Both the moisture and heat flux have a term containing the condensation or evaporation rate. Rayleigh damping reduces the moisture flux, while the heat flux is enhanced by diabatic forcing during precipitating events. In magnitude, A is significantly larger than the B coefficient associated with the forcing in the sensible heat flux equations given in the Appendix.

TABLE 1. A scale analysis* of the terms in the u moisture wind [Eq. (8)].

	$\frac{d(qu)}{dt}$	qfv	$\frac{q}{\rho}\frac{\partial p}{\partial x}$	Aqu
Scaling	$\frac{qU^2}{L}$	$q2\Omega U$	$\frac{q}{\rho}\frac{\Delta p}{L}$	$\frac{U^2q}{L_c}$
Magnitude				
(extratropics)	$q \times 10^{-4}$	$q \times 10^{-3}$	$q \times 10^{-3}$	$\leqslant q \times 10^{-3}$
(tropics)	$q \times 10^{-4}$	$\leqslant q \times 10^{-4}$	$q \times 10^{-3}$	$\leqslant q \times 10^{-3}$

* $U \sim 10$ m s^{-1}, $A \sim \frac{U}{L_c}$ s^{-1}, $L \sim 10^6$ m, L_c (precipitation scale) $\gtrsim 10^5$ m, $\Delta p \sim 10^3$ N m^{-2}.

analysis for (6) and (7) the term containing diabatic processes is an order of magnitude more important than the contribution from the total derivative, provided A is scaled with Q proportional to 10^{-7} g g^{-1} s^{-1}, a magnitude common to mesoscale precipitation events. Table 1 illustrates our findings for large-scale circulations containing a long-lived mesoscale diabatic process, of length scale L_c, for tropical and nontropical situations. In Table 1 the derivative term yields a magnitude U^2q/L, while the diabatic term gives U^2q/L_c, where Q is scaled by Uq/L_c and $L_c = 10^5$ m. In tropical regions the Coriolis parameter is reduced; thus, the pressure gradient and the damping terms dominate provided A is sufficiently large. This scale analysis suggests that the large-scale fluid flow is nearly balanced by the right-hand sides in (6) and (7). This is consistent with our stated hypothesis. Clearly, different scaling will provide different magnitudes; for example, short duration or microscale diabatic processes are of much less importance to the large-scale flow. However, the Rayleigh damping term remains important provided $L_c/L \sim 0.1$. Convective parameterizations assume a similar ratio between grid and diabatic scales. However, the total derivative in (10) and (11) becomes important as the scale size is reduced.

In this study (10) and (11) or (6) and (7) are evaluated *diagnostically*. The right-hand sides of these equations are assumed to be nearly in balance, but some contribution from the total derivative is allowed. A simplified analysis is used to trace how the nonconservative total derivative contributes. As an example, assume that the deviation from conservation is known to be a small fraction of the flux; then for nonzero values of q, u, and v there exist coefficients α_u and α_v such that

$$\frac{d(qu)}{dt} = \alpha_u qu, \tag{12}$$

$$\frac{d(qv)}{dt} = \alpha_v qv. \tag{13}$$

This is a generalization of the approximation for the partial time derivative used in Gill (1980) and Matsuno (1966). To get a grasp of the magnitude of the coefficient assume that the flux qu experiences a complete reversal of sign for the synoptic flow within a time period of Δt; then the coefficient α_u would have magnitude $2/\Delta t$. Generally the magnitude is less than this. The coefficients α_u and α_v, however, are locally functions of time and the independent spatial variables. For long-lived large-scale diabatic situations these coefficients vary slowly in space. Within mesoscale disturbances they should vary in a pattern consistent with the disturbance. For example, the convection may moisten the upper atmosphere, giving α_u and α_v a positive sign, while drying lower levels making the coefficients negative. Equations (12) and (13) allow a climatological estimate of the nonconservative property of the horizontal kinematic moisture fluxes to be easily determined from model calculations. A more complete solution procedure that makes no simplifying assumptions will be presented elsewhere in an independent study.

Substituting (12) and (13) into (10) and (11) gives

$$-fv_g + fv + u(A - \alpha_u q) = 0, \tag{14}$$

$$fu_g - fu + v(A - \alpha_v q) = 0. \tag{15}$$

Note that A, $\alpha_u q$, and $\alpha_v q$ couple the two algebraic equations together. Dividing (14) and (15) by f and solving the coupled system for u and v yields

$$u_m \equiv u = \frac{u_g + M_v v_g}{1 + M_u M_v}, \tag{16}$$

$$v_m \equiv v = \frac{v_g - M_u u_g}{1 + M_u M_v}. \tag{17}$$

Here the subscript m denotes the moist solution. Note that $u_m = u_g$ and $v_m = v_g$ when $M_u \equiv (A - \alpha_u)f^{-1}$ and $M_v \equiv (A - \alpha_v)f^{-1}$ are set to zero. Here A is negative for condensation, so a positive value of α_u and α_v would enhance the magnitude of M_u and M_v. For some circumstances—for example, for large hourly condensation rates in a hurricane—the magnitude of the nondimensional number $R_1 \equiv Af^{-1}$ can exceed unity. A condensation rate of $Q \approx -0.8 \times 10^{-7}$ g g^{-1} s^{-1} yields $R_1 = -0.408$, provided $f = 10^{-4}$ and an average q satisfies $q = 2$ g kg^{-1}. Magnitudes for R_1 of 0.2 and less, however, are probably more common for large areas.

For tropical flow the moist wind is computed using (6), (7), (12), and (13). This yields

$$u_m \equiv u = \left(-\frac{1}{\rho}\frac{\partial p}{\partial x}\right)\left(\frac{1}{\alpha_u - A}\right), \tag{18}$$

$$v_m \equiv v = \left(-\frac{1}{\rho}\frac{\partial p}{\partial y}\right)\left(\frac{1}{\alpha_v - A}\right), \tag{19}$$

provided neither $\alpha_u - A$ nor $\alpha_v - A$ is equal to zero. The perturbation in the horizontal velocity is found

using the pressure gradient computed from the diabatic heating. If the total derivative term; that is, in (6) and (7) is small, then the perturbation flow induced by the diabatic process is antitriptic; that is, there is a near balance between the Rayleigh damping term and the pressure gradient term. An example of antitriptic flow is found in Raymond (1986), illustrating topographically induced mesoscale circulations in barotropic flow around an isolated mesoscale obstacle. Similar circulations containing positive and negative couplet pairs of convergence–divergence and cyclonic–anticyclonic flows are produced by this antitriptic mechanism.

For extratropical flow an examination of (16) and (17) expanded in powers of R_1 provides a clearer picture. Assuming that $u_m = u_L + u_{\text{pert}}$ and $v_m = v_L + v_{\text{pert}}$, where u_L and v_L are the horizontal wind components in the large-scale flow, and assigning all terms involving Q to the perturbation, yields for the perturbation and large-scale flow the expressions

$$u_{\text{pert}} = R_1 v_g - R_1^2 u_g + \frac{R_1(\alpha_u + \alpha_v)u_g}{f} + \cdots, \quad (20a)$$

$$u_L = u_g - \frac{\alpha_v v_g}{f} + \frac{\alpha_u \alpha_v u_g}{f^2} + \cdots, \quad (20b)$$

$$v_{\text{pert}} = -R_1 u_g - R_1^2 v_g + \frac{R_1(\alpha_u + \alpha_v)v_g}{f} + \cdots, \quad (21a)$$

$$v_L = v_g + \frac{\alpha_u u_g}{f} - \frac{\alpha_u \alpha_v v_g}{f^2} + \cdots. \quad (21b)$$

Note that the large-scale flow is nearly balanced if $|\alpha_v|/f \ll 1$ and $|\alpha_u|/f \ll 1$. Also the series in (20b) and (21b) converge rapidly, provided these ratios are much less than 1. When this is not the case, this series expansion should not be used.

In the Northern Hemisphere, given $R_1 < 0$ (condensation) with $u_g > 0$ and $v_g > 0$, (20a) and (21a) imply that the magnitude of a westerly flow is reduced, since $u_g/u_m > 1$, while the magnitude of a southerly flow is enhanced, since $v_g/v_m < 1$. Repeating this thought experiment with an easterly flow leads to the reverse conclusions. In the Southern Hemisphere, $u_g > 0$ implies that a northerly flow is enhanced because the coriolis parameter changes sign making $R_1 > 0$. As will be shown in the hurricane example given below, the diabatic perturbation terms [(20a) and (21a)] add significantly to the local convergence.

The diabatic contribution alters the speed $V_m = (u_m^2 + v_m^2)^{1/2}$. Writing the definition of speed in terms of the large-scale wind and the diabatic perturbation gives

$$V_m = [V_L^2 + 2u_L u_{\text{pert}} + 2v_L v_{\text{pert}} + (u_{\text{pert}})^2 + (v_{\text{pert}})^2]^{1/2}. \quad (22a)$$

Here $V_L = (u_L^2 + v_L^2)^{1/2}$. Approximating the large-scale flow by factoring out V_L but replacing all occurrences of V_L in the denominator by V_g yields

$$V_m = V_L\left[1 + 2\left(\frac{u_L}{V_g^2}\right)u_{\text{pert}} + 2\left(\frac{v_L}{V_g^2}\right)v_{\text{pert}} + \left(\frac{u_{\text{pert}}}{V_g}\right)^2 + \left(\frac{v_{\text{pert}}}{V_g}\right)^2\right]^{1/2}, \quad (22b)$$

where $V_g = (u_g^2 + v_g^2)^{1/2}$. Substituting from (20) and (21) into (22b) gives

$$V_m = V_g\left[1 - R_1^2 + \frac{2R_1(\alpha_u + \alpha_v)}{f} - \frac{2R_1(\alpha_u u_g^2 + \alpha_v v_g^2)}{fV_g^2} + \frac{2R_1 u_g v_g(\alpha_v - \alpha_u)}{fV_g^2} + \frac{2R_1 u_g v_g(\alpha_u + \alpha_v)(\alpha_v - \alpha_u)}{f^2 V_g^2} + \cdots\right]^{1/2} + \cdots. \quad (22c)$$

Note that $V_m = V_g(1 - R_1^2)^{1/2}$ when $\alpha_u = \alpha_v = 0$. All terms in the brackets except for the first two tend to nullify each other or make small contributions provided $|\alpha_v|/f \ll 1$ and $|\alpha_u|/f \ll 1$. Thus, (22c) implies that the speed associated with moist cyclonic activity is less than the geostrophic value.

For comparison purposes, note that the relationship between the geostrophic and gradient wind speed V_{gr} is

$$V_{\text{gr}} = V_g\left(1 + \frac{V}{fR}\right)^{-1}, \quad (23)$$

where R is the radius of curvature (Holton 1979). For cyclonic situations ($fR > 0$) the ratio V_{gr}/V_g is less than 1. Thus, the speed is reduced from geostrophic values by the gradient wind primarily because curvature effects are included. In regions having condensation, the rate needed to sustain a specific curvature can be determined approximately by equating (22c) and (23), and solving for Q. Approximating the solution by the first two terms in (22c) gives

$$Q = -fq\left[1 - \left(1 + \frac{V}{fR}\right)^{-2}\right]^{1/2}. \quad (24)$$

As an example, if $f = 10^{-4}$, $V/fR = 0.2$, and $q = 2$ g kg^{-1}, then $Q = -1.1055 \times 10^{-7}$ g g^{-1} s^{-1}. Note that Q is proportional to fq.

3. An example

Idealized flow in a hurricane is used to illustrate the diabatic influence on the wind field. An idealized axisymmetric vortex flow was selected because of its interesting theoretical properties and because of the initialization difficulties encountered when inserting a diabatic vortex flow in a numerical model. Following the procedure presented in section 2, but for cylindrical

coordinates and for axisymmetric flow, allows the moist radial wind component u_m to be written in terms of the tangential velocity v according to

$$u_m = vM_v\left(1 + \frac{v}{fr}\right)^{-1}. \tag{25}$$

It is assumed that the contribution from $\alpha_v f^{-1}$ in M_v is small. Near the vortex core $v/fr \gg 1$; thus, u_m simplifies to

$$u_m = frM_v, \tag{26}$$

while far from the core $v/fr \ll 1$, so

$$u_m = vM_v. \tag{27}$$

The divergence is

$$\frac{\partial u_m}{\partial r} + \frac{u_m}{r} = M_v\left(1 + \frac{v}{fr}\right)^{-1}\left(\frac{\partial v}{\partial r} + \frac{v}{r}\right) + v\left(1 + \frac{v}{fr}\right)^{-1} \times \frac{\partial M_v}{\partial r} - M_v\left(1 + \frac{v}{fr}\right)^{-2}\left(\frac{\partial v}{\partial r} - \frac{v}{r}\right)\frac{1}{fr}. \tag{28}$$

For $v/fr \gg 1$, the divergence [(28)] simplifies to

$$\frac{\partial u_m}{\partial r} + \frac{u_m}{r} = 2fM_v + \frac{rf\partial M_v}{\partial r}, \tag{29a}$$

while when $v/fr \ll 1$ the expression is

$$\frac{\partial u_m}{\partial r} + \frac{u_m}{r} = M_v\left(\frac{\partial v}{\partial r} + \frac{v}{r}\right) + \frac{v\partial M_v}{\partial r}. \tag{29b}$$

In (29a) the sign depends upon M_v and its radial variation. In (29b) the divergence depends upon the vorticity $(\partial v/\partial r + v/r)$ and the radial variation in M_v. In both (29a) and (29b) $M_v < 0$ contributes toward the convergence, provided the magnitude of M_v is increasing radially outward and $v > 0$. Positive vorticity, averaged over the hurricane inner core, of $10^{-2}\ s^{-1}$ is common. Thus, as indicated by (29), substantial convergence is generated by diabatic processes when M_v is sufficiently large in magnitude and of negative sign. Negative vorticity with $M_v < 0$ and decreasing outward implies divergence. Evaporation near the cloud tops also encourages divergence.

To express the radial velocity as a function of distance from the vortex center, it is necessary to know M_v, or Q when $\alpha_v f^{-1}$ is small, and its radial distribution. Near the vortex center a constant value for M_v would imply, following (27), a flow that is proportional to r (solid rotation), while if M_v were linear in r, then u would be proportional to r^2. Far from the vortex center the radial component [(28)] is proportional to the tangential component v and to M_v. In the outer reaches of a hurricane the radial distribution of v decreases approximately as $r^{-1/2}$ (Riehl 1963). Thus, the radial variation in u_m is considerable but depends a great deal upon the radial variation of the net condensation rate Q.

In the absence of condensation or evaporation ($Q = 0$) our solutions satisfy $u = 0$ unless $\alpha_v \neq 0$. Thus, radial velocities associated with condensation bands in hurricanes should be localized and exist in addition to a dynamically induced large-scale convergence associated with $\alpha_v \neq 0$. These bands in the radial velocity are seen in both numerical model simulations and in observations of hurricanes (Willoughby 1979).

With a balance between the centrifugal and pressure gradient forces that characterizes intense atmospheric vortices, cyclostrophic flow leads to a tangential velocity defined by

$$v_c = \left(\frac{r}{\rho}\frac{\partial p}{\partial r}\right)^{1/2}. \tag{30}$$

Therefore, solving for the moist tangential velocity $v_m = v$, in the cylindrical moisture flux equations, using a procedure analogous to that developed in earlier sections, gives

$$v_m^2 + frv_m + fru_mM_u = v_c^2. \tag{31}$$

Ignoring the dependence of u_m on v_m yields a moisture-modified gradient wind expression

$$v_m = -\frac{fr}{2} \pm \frac{fr}{2}\left[1 - \frac{4u_mM_u}{fr} + \frac{4v_c^2}{(fr)^2}\right]^{1/2}. \tag{32}$$

Retaining the dependence of v_m on u_m developed above [(25)] requires solving the cubic equation

$$v_m^3 + 2frv_m^2 + [(1 + M_vM_u(fr)^2 - v_c^2]v_m = frv_c^2 \tag{33}$$

for v_m. Note that (33) remains cubic even when $M_v = M_u = 0$, implying than an extraneous real root[2] has been introduced by the algebra.

Results are presented in Fig. 1 to illustrate the differences between (32) and (33). The axisymmetric tangential flow is taken from the analytical expression given in (6) of Fiorino and Elsberry (1989), with maximum velocity $V_{max} = 35\ m\ s^{-1}$. In their formula for the tangential wind the radius of maximum tangential winds is set to $r_{max} = 100$ km and the parameter $b = 0.96$. For simplicity, in our experiments this radial profile is assumed to be in cyclostrophic balance, and is illustrated by the thick line in Fig. 1. Adding the influence of the Coriolis parameter (gradient wind) for a dry case [$u_m = 0$, (32)] produces reductions in the tangential velocity of approximately 4 m s^{-1} at r_{max}, with larger values outside the radius of maximum winds. Willoughby (1990) indicates that the gradient balance condition closely approximations the axisymmetric tangential winds observed in hurricanes. However, it should be remembered that measured pressure

[2] For the v_c used, (33) has three real roots, two of which are negative.

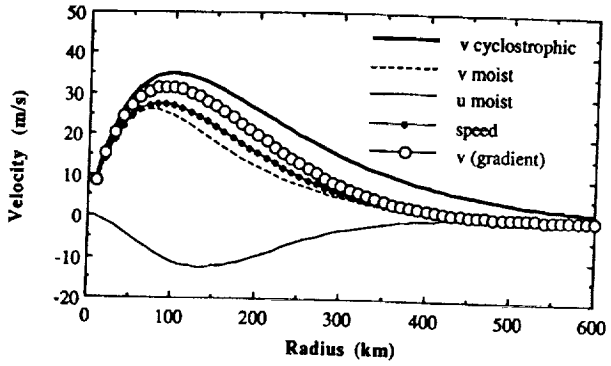

FIG. 1. Idealized axisymmetric hurricane cyclostrophic, gradient, and moist tangential velocities (m s^{-1}) as a function of radius. Speed and radial component also illustrated for the moist wind.

gradients already contain diabatic contributions. This could explain the discrepancy between these observational findings (Willoughby 1990) and the theoretical and numerical findings that intense vortices react strongly to specified heat sources (Hank and Schubert 1986; Delden 1989). Note that our moist wind solution, as illustrated by the divergence in (29), is also dependent upon the intensity of the vortex.

To solve (33) for v_m, the nondimensional values of M_v and M_u (Fig. 2) are assigned to be proportional to v_c so that each is -2 at r_{max}. This large magnitude for M_v and M_u is used to dramatize the response of the drag terms. The roots of (33) give one real positive solution for v_m that can be used to evaluate (25), yielding a radial inflow of approximately 12 m s^{-1}. As expected, the diabatic influence reduces the speed and shifts the radius of maximum tangential velocity from 100 to 80 km, while generating the maximum magnitude of the radial velocity at r = 140 km. The maximum reduction in the tangential velocity component is about 8 m s^{-1}, but the overall reduction in the speed is less since a strong radial inflow is present. Considering that our estimates of M_v and M_u are inflated in magnitude and in areal coverage, we can probably infer that the tangential velocities are not greatly altered by the diabatic drag term.

Magnitudes of M_v and M_u dictate the radius of maximum heating (RMH). Figure 2 shows a curve for $M = M_v = M_u$ where the RMH is at 100 km, and another M that is positive between 0 and 50 km, illustrating possible modifications (exaggerated) because of inner core evaporation. These M's are used in the calculation of u_m to show the importance of the divergence as a function of the RMH, as illustrated in Fig. 3. In every case the balanced solutions show that the greatest convergence is located interior to the circle with the prescribed RMH. Whether this would result in a change in the location of the RMH depends on the availability of moisture and other factors. However, in these calculations the radius of the maximum cyclostrophic wind was held fixed at 100 km. Otherwise, little change occurs in the magnitude or location of the maximum value of v_m as a function of RMH.

Observations or results from model simulations of intense vortices are needed to complete the evaluation of the moisture-modified horizontal winds and the evaluation of the diabatic and total derivative terms. The contribution from the total derivative would be expected to vary spatially, but the pattern should be consistent between similar types of situations and should change in time somewhat slowly.

4. Applications

Cumulus initialization and parameterization of long-lived convection in the extratropics are areas that could benefit from the knowledge contained in (16), (17), (18), and (19). The following discussion highlights some simple tests to investigate this potential in cumulus parameterization. These tests are presented to illustrate possible applications and do not represent a completely definitive study of the topic.

Cumulus parameterization schemes—for example, Kuo (1965, 1974)—estimate subgrid-scale moist con-

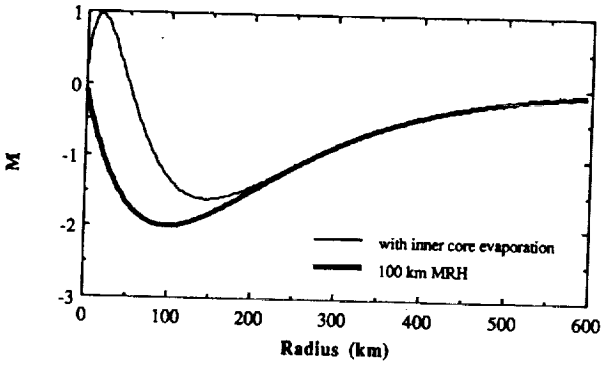

FIG. 2. Radial profiles of M illustrating (exaggerated) radial distribution of the condensation or evaporation rate.

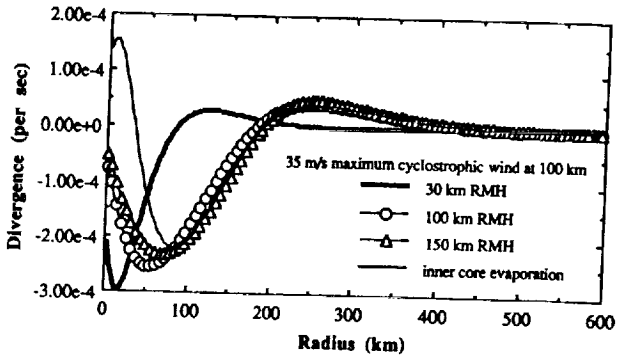

FIG. 3. Radial distribution of the moist divergence (s^{-1}) as a function of M.

vective activity using the instantaneous state of the grid-scale variables and moisture or cloud properties. This information is then used to modify the large-scale temperature and moisture fields. Because cumulus clouds contain a large vertical component of motion, relative to their environment, they also are responsible for significant vertical momentum transport. Several schemes based on cumulus friction concepts have been introduced to adjust the grid-scale momentum (Ooyama 1971; Shapiro and Stevens 1973; Schneider and Lindzen 1967; Shapiro and Stevens 1980; Zhang and Cho 1991). These approaches introduce a cloud velocity that requires an additional determination, usually from a cloud model. In contrast, the terms in (20a) and (21a) that represent approximate changes in the large-scale wind introduce no cloud-scale dependent variables but require calculation of the geostrophic wind.

To test the momentum adjustment suggested by the perturbation terms in (20a) and (21a), they were added to the Kuo cumulus parameterization scheme in the local [Cooperative Institute for Meteorological Satellite Studies (CIMSS)] version of the Australian Bureau of Meteorology Research Centre's (BMRC) finite-area model (Leslie et al. 1985). Thus, $u_{new} = u_{old} + u_{pert}$ where (20a) defines u_{pert}; similarly, $v_{new} = v_{old} + v_{pert}$ where (21a) defines v_{pert}. Our configuration of this semi-implicit regional model has 15 sigma levels. A 12-h control forecast, 0000–1200 UTC 22 April 1988, with 150-km horizontal resolution and 600-s time steps was performed using the standard Kuo cumulus parameterization scheme (1965) without any momentum adjustment. In the test forecast the first two terms in (20a) and (21a) are used to modify the horizontal wind components u and v, with the added requirement that $|R_i| < 0.5$. (Smaller magnitudes for R_i may be more acceptable.) This large magnitude for R_i was used to highlight the differences between the two schemes in a short forecast. Even though the convection may vary slightly in location and intensity between model time steps, it is still assumed that the convection is long lived. Spatially isolated convection will not result in introducing numerical noise because such noise is removed efficiently by the high-order low-pass tangential or sine filters (Raymond 1988; Raymond and Garder 1991). In Fig. 4 the differences between the forecasts for the 500-mb mixing ratios (g kg^{-1}) are superimposed upon the infrared satellite image. Note that small increases in the mixing ratio occur over cloudy regions,

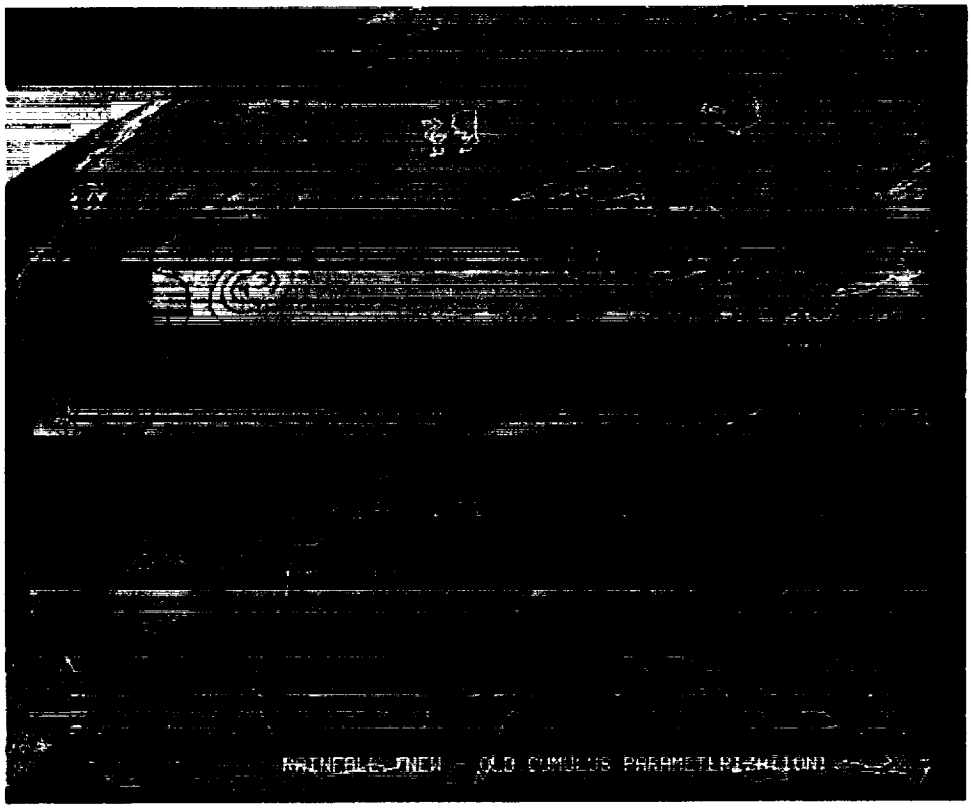

FIG. 4. Difference (×10) in the mixing ratio (g kg^{-1}) for a 12-h forecast (0000–1200 UTC 22 April 1988) with and without the perturbation wind [Eqs. (20a) and (21a)] application in the cumulus cloud parameterization scheme. Differences are superimposed upon the VAS infrared image.

but decreases occur over regions associated with descending vertical motion. In this figure the band of clouds to the north and west is associated with a cold front, while the band over the Gulf coast is high clouds streaming in over Mexico from the Pacific Ocean. (These bands are separated by a strong wind jet.) Our tests show that the first term in (20a) and (21a) is responsible for most of enhanced vertical circulation.

The convective rainfall from the cumulus scheme with momentum adjustment was slightly less than that produced by the traditional Kuo procedure because the restriction $|R_1| < 0.5$ limited the amount of condensation. This made the parameterization more realistic since too much condensation was occurring too rapidly in some localities with the standard scheme. It is known—for example, Krishnamurti et al. (1980)—that the original Kuo (1965) scheme gives excessive moistening of the atmosphere. Sundqvist et al. (1989) introduced a special factor to govern the vertical distribution of convective heating to help correct that problem. Nevertheless, a maximum increase in the nonconvective rainfall of 4 mm in 12 h was also observed. This increase (Fig. 5) occurred because of the enhanced vertical circulation that resulted from the application of the momentum adjustment [(20a) and (21a)].

Initialized National Meteorological Center global analyses valid over North America between 1200 UTC 9 March and 1200 UTC 12 March 1988 were used as initial and boundary conditions in a 72-h forecast made by the CIMSS regional model using 190.5-km resolution on a 41 × 37 horizontal grid with a 720-s time step. The control forecast uses no momentum adjustment. In the test case the momentum adjustment uses the first two terms given in (20a) and (21a) with the restriction that $|R_1| < 0.25$. Also, the sixth-order implicit tangent filter (Raymond 1988) is applied with a filter factor of either $\epsilon = 0.05$ or $\epsilon = 0.64$. The latter value gives moderate to heavy filtering. The u velocity component rms differences between verifying initialized analysis and forecast are shown as a function of time in Figs. 6a–c. The momentum adjustment at sigma level 3 (approximately 230 mb) results in a small improvement in the statistics except at 24 h. Increasing the filter factor from 0.05 to 0.64 has a larger impact than the adjustment, primarily because all grid points are involved. In contrast, the maximum number of occurrences for cumulus parameterization is no more

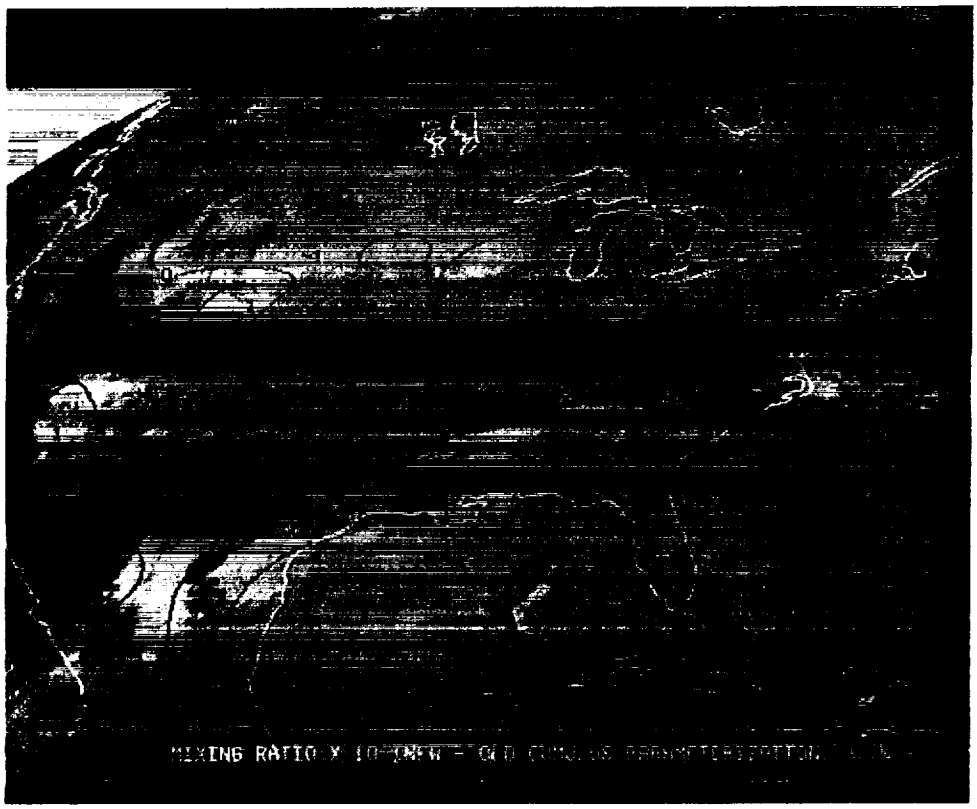

FIG. 5. Same as Fig. 4 but illustrating the 12-h difference in the total rainfall (mm) between the two 12-h forecasts.

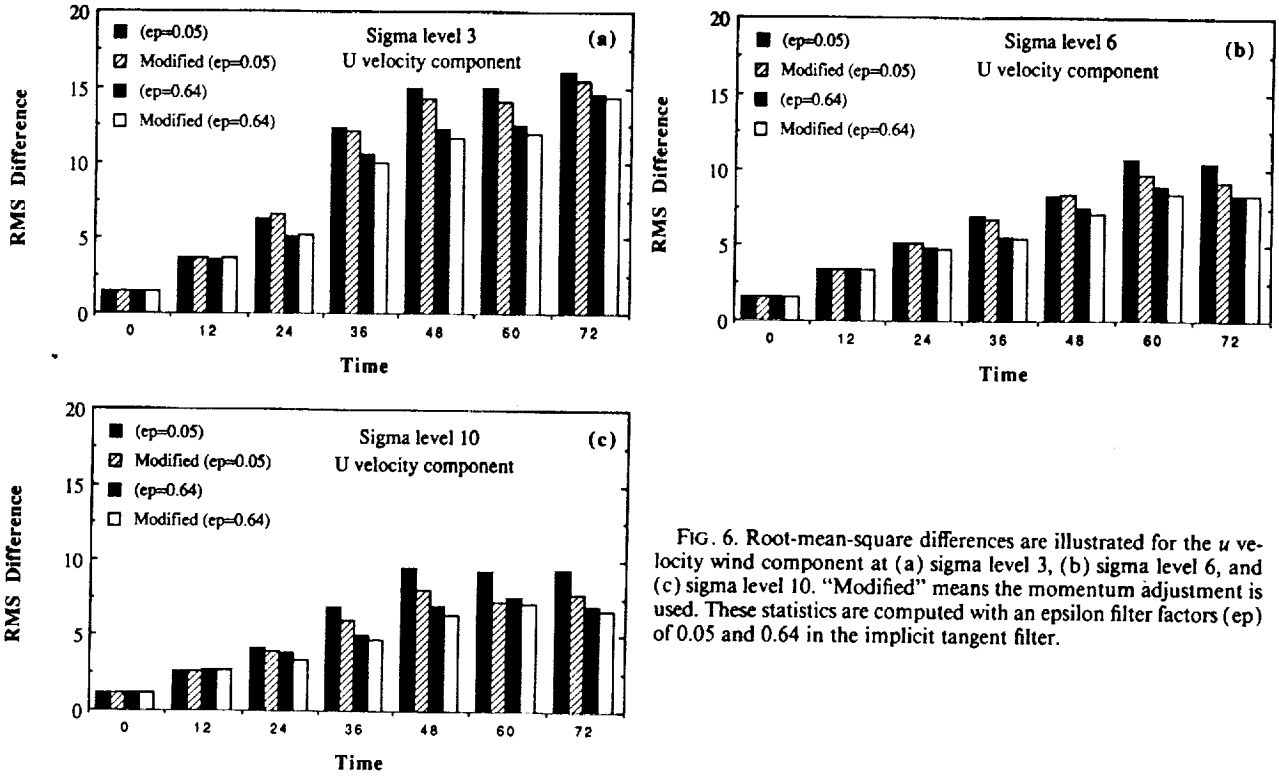

FIG. 6. Root-mean-square differences are illustrated for the u velocity wind component at (a) sigma level 3, (b) sigma level 6, and (c) sigma level 10. "Modified" means the momentum adjustment is used. These statistics are computed with an epsilon filter factors (ep) of 0.05 and 0.64 in the implicit tangent filter.

than 527 vertical profiles out of about 1500 possible locations (see Fig. 8). At sigma level 6 (Fig. 6b, approximately 440 mb) the major improvement occurs late in the forecast. Lower levels (approximately 720 mb) respond best to the momentum adjustment, as illustrated in Fig. 6c. In all cases, heavy filtering always reduces the contribution from the adjustment. The v velocity wind component rms differences are shown in Fig. 7. Again, sigma level 10 shows the most improvement at 60 and 72 h. Upper-level contributions average out to near neutral or slightly on the negative side. This may reflect shortcomings in the cumulus parameterization or in the momentum adjustment process or in both. The lack of entrainment or vertical mixing by turbulence in the cumulus parameterization is clearly a deficiency. How case dependent the adjustment procedure is remains unknown, as do estimates for α_u and α_v.

The number of active cumulus parameterizations versus time step is shown for a 36-h period in Fig. 8. It shows that cumulus convective activity is slightly enhanced early in the forecast and experiences less $2\Delta t$ and other high-frequency oscillations with the momentum adjustment.

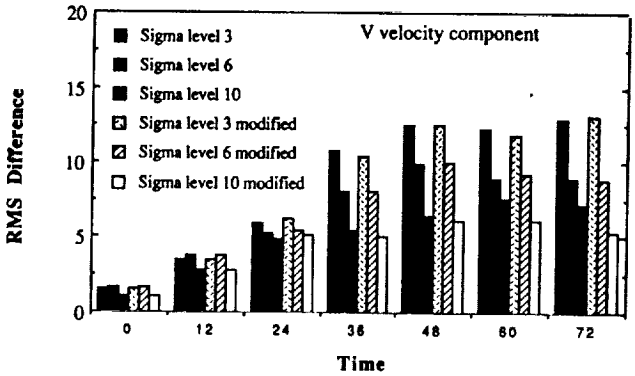

FIG. 7. Same as Fig. 6 but for the v velocity wind component and with the smaller filter factor.

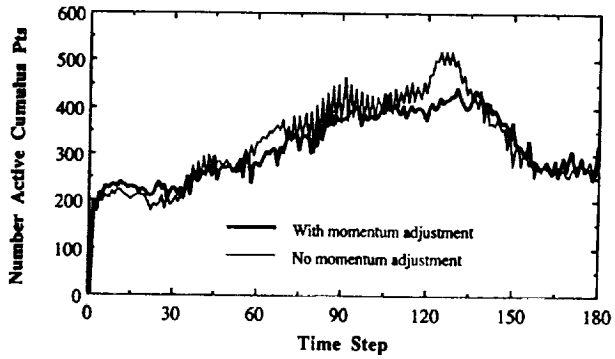

FIG. 8. Number of grid points experiencing cumulus parameterization as a function of the time step.

5. Summary

A diabatically induced term is present in the equations describing the moisture flux and heat flux. This term has the form of damping (forcing) for condensation (evaporation). Diabatic processes also influence the horizontal flux through the pressure gradient term. In this study the influence of the damping term is evaluated, but the characteristics associated with diabatic changes to the geostrophic wind are not analyzed.

This study finds that mild reductions in the large-scale wind speed caused by cumulus friction can contribute to the near conservation of the large-scale horizontal components of the moisture flux. This is the consequence of an establishment of a near balance between the pressure gradient, Coriolis, and Rayleigh damping terms in the moisture flux equations. This balance is identified by scale analysis. This outcome is independent of the mechanism responsible for the reduction in wind speed.

Estimates of diabatically related changes to the horizontal wind are easily obtained from the balanced relationship. For realistic condensation rates, these wind estimates are consistent with the gradient wind approximation. When these estimates are used in a simple hurricane model they predict a radial inflow with convergence, provided the rotation is cyclonic. In contrast, divergence is associated with anticyclonic rotation and evaporation. When the predicted wind perturbations are used as a momentum adjustment in a Kuo cumulus parameterization scheme they improve the 72-h forecast rms u velocity component error statistics and enhance mesoscale vertical circulations. In the tropics any movement toward conservation of moisture flux enhances an antitriptic relationship, cementing a near balance between a Rayleigh damping term and the pressure gradient term. Note that it is necessary to have the condensation before the wind-related processes can be activated. In this way this process is similar to conditional instability of the second kind (CISK).

Our equations (20a) and (21a) are approximations of the influence from one diabatic source on the wind. A more rigorous study using the vorticity and divergence concept will be described elsewhere. The terms in the flux equations are also being analyzed using mesoscale model calculations. This is the subject of continuing study.

Acknowledgments. This work was supported by National Science Foundation ATM-8920508 and NASA NAGW-1855. The author thanks Arthur Garder (Professor Emeritus, Southern Illinois University, Edwardsville, Illinois), Barry Hinton (SSEC, University of Wisconsin), and Robert Rabin (NSSL, Normal, Oklahoma) for helpful suggestions. Leo Donner (GFDL, Princeton, New Jersey), Robert Merrill (CIMSS, University of Wisconsin), and Franklin Robertson (NASA/Marshall, Huntsville, Alabama) are thanked for suggesting specific references.

APPENDIX

The Sensible Heat Flux Equations

The equations describing the temporal and spatial distribution of the horizontal components of the sensible heat flux can be constructed from (1), (2), and (4). They are

$$\frac{d(\theta u)}{dt} = -\frac{\theta}{\rho}\frac{\partial p}{\partial x} + \theta f v - B\theta u, \qquad \text{(A1)}$$

$$\frac{d(\theta v)}{dt} = -\frac{\theta}{\rho}\frac{\partial p}{\partial y} - \theta f u - B\theta v. \qquad \text{(A2)}$$

In these equations the damping coefficient $B = LQ/(Tc_p)$; here, T is temperature, c_p is the specific heat at constant pressure, and L is the latent heat of vaporization. For condensation processes B is negative but smaller in magnitude than the coefficient A in (8) and (9).

REFERENCES

Austin, P. M., and R. A. Houze, 1973: A technique for computing vertical transports by precipitating cumuli. *J. Atmos. Sci.*, **30**, 1100–1111.

Cho, H. R., 1985: Rates of entrainment and detrainment of momentum of cumulus clouds. *Mon. Wea. Rev.*, **113**, 1920–1932.

Daley, R., 1991: *Atmospheric Data Analysis.* Cambridge University Press, 457 pp.

Delden, A. van, 1989: On the deepening and filling of balanced cyclones by diabatic heating. *Meteor. Atmos. Phys.*, **41**, 127–145.

Donner, L. J., 1988: An initialization for cumulus convection in numerical weather prediction models. *Mon. Wea. Rev.*, **116**, 377–385.

——, H. L. Kuo, and E. J. Pitcher, 1982: The significance of thermodynamic forcing by cumulus convection in a general circulation model. *J. Atmos. Sci.*, **39**, 2159–2181.

Esbensen, S. K., L. J. Shapiro, and E. I. Tollerud, 1987: The consistent parameterization of the effects of cumulus clouds on the large-scale momentum and vorticity fields. *Mon. Wea. Rev.*, **115**, 664–669.

Fiorino, M., and R. L. Elsberry, 1989: Some aspects of vortex structure related to tropical cyclone motion. *J. Atmos. Sci.*, **46**, 975–990.

Gill, A. E., 1980: Some simple solutions for heat-induced tropical circulations. *Quart. J. Roy. Meteor. Soc.*, **106**, 447–462.

Hack, J. J., and W. H. Schubert, 1986: Nonlinear response of atmospheric vortices to heating by organized cumulus convection. *J. Atmos. Sci.*, **43**, 1559–1573.

Haltiner, G. J., and R. T. Williams, 1980: *Numerical Prediction and Dynamic Meteorology.* Wiley, 477 pp.

Heckley, W. A., and A. E. Gill, 1984: Some simple analytical solutions to the problem of forced equatorial long waves. *Quart. J. Roy. Meteor. Soc.*, **110**, 203–217.

Holton, J. R., 1979: *An Introduction to Dynamic Meteorology.* Academic Press, 391 pp.

——, and D. E. Colton, 1972: A diagnostic study of the vorticity balance at 200 mb in the tropics during the northern summer. *J. Atmos. Sci.*, **29**, 1124–1128.

Houze, R. A., and P. V. Hobbs, 1982: Organization and structure of precipitating cloud systems. *Advances in Geophysics*, No. 24, Academic Press, 225–315.

Konig, W., and E. Ruprecht, 1989: Effects of convective clouds on the large-scale vorticity budget. *Meteor. Atmos. Phys.*, **41**, 213–229.

Krishnamurti, T. N., S. Low-Nam, and R. Pasch, 1983: Cumulus parameterization and rainfall rates II. *Mon. Wea. Rev.*, **111**, 815–828.

——, K. Ingles, S. Cocke, T. Kitade, and R. Pasch, 1984: Details of low latitude medium range numerical weather prediction using a global spectral model. *J. Meteor. Soc. Japan*, **62**, 613–648.

——, Y. Ramanathan, H.-L. Pan, R. J. Pasch, and J. Molinari, 1980: Cumulus parameterization and rainfall rates. *Mon. Wea. Rev.*, **108**, 456–464.

Kuo, H. L., 1965: On formation and intensification of tropical cyclones through latent heat release by cumulus convection. *J. Atmos. Sci.*, **22**, 40–63.

——, 1974: Further studies of the parameterization of the influence of cumulus convection on large-scale flow. *J. Atmos. Sci.*, **31**, 1232–1240.

Kuo, Y. H., and R. S. Reed, 1988: Numerical simulation of an explosively deepening cyclone in the eastern Pacific. *Mon. Wea. Rev.*, **116**, 2081–2105.

Leslie, L. M., G. A. Mills, L. W. Logan, D. J. Gauntlett, G. A. Kelly, J. L. Mcgregor, and M. J. Manton, 1985: A high resolution primitive equation NWP model for operations and research. *Aust. Meteor. Mag.*, **33**, 11–35.

Lorenz, E. N., 1978: Available energy and the maintenance of a moist circulation. *Tellus*, **30**, 14–31.

Malkus, J. S., 1952: The slopes of cumulus clouds in relation to external wind sheer. *Quart. J. Roy. Meteor. Soc.*, **78**, 530–542.

Matsuno, T., 1966: Quasi-geostrophic motions in the equatorial area. *J. Meteor. Soc. Japan*, **44**, 25–43.

Ooyama, K., 1971: Convection and convection adjustment: A theory on parameterization of cumulus convection. *J. Meteor. Soc. Japan*, **49** (special issue), 744–756.

Petterssen, S., 1956: *Weather Analysis and Forecasting*. McGraw-Hill, 428 pp.

Raymond, W. H., 1986: Topographical-induced mesoscale motions in antitriptically balanced barotropic flow. *Tellus*, **38A**, 251–262.

——, 1988: High-order low-pass implicit tangent filters for use in finite area calculations. *Mon. Wea. Rev.*, **116**, 2132–2141.

——, and A. Garder, 1991: A review of recursive and implicit filters. *Mon. Wea. Rev.*, **119**, 477–495.

Reed, R. J., A. J. Simmons, M. D. Albright, and P. Unden, 1988: The role of latent heat release in explosive cyclogenesis: Three examples based on ECMWF operational forecasts. *Wea. Forecasting*, **3**, 217–229.

Riehl, H., 1963: Some relations between the wind and thermal structure of steady-state hurricanes. *J. Atmos. Sci.*, **20**, 276–287.

——, 1979: *Climate and Weather in the Tropics*. Academic Press, 611 pp.

——, and J. S. Malkus, 1958: On the heat balance of the equatorial trough zone. *Geophysica*, **6**, 503–538.

Schneider, E. K., and R. S. Lindzen, 1976: A discussion of the parameterization of momentum exchange by cumulus convection. *J. Geophys. Res.*, **81**, 3158–3160.

Shapiro, L. J., and D. E. Stevens, 1980: Parameterization of convective effects on the momentum and vorticity budgets of synoptic-scale Atlantic tropical waves. *Mon. Wea. Rev.*, **108**, 1816–1826.

Stull, R. B., 1988: *An Introduction to Boundary Layer Meteorology*. Kluwer Academic Publishers, 666 pp.

Sui, C. H., and M. Yanai, 1986: Cumulus ensemble effects on the large-scale vorticity and momentum fields of GATE. Part I: Observational evidence. *J. Atmos. Sci.*, **43**, 1618–1642.

Sundqvist, H., E. Berge, and J. E. Kristjansson, 1989: Condensation and cloud parameterization studies with a mesoscale numerical weather prediction model. *Mon. Wea. Rev.*, **117**, 1641–1657.

Tarbell, T. C., T. T. Warner, and R. A. Anthes, 1981: An example of the initialization of the divergent wind component in a mesoscale numerical weather prediction model. *Mon. Wea. Rev.*, **109**, 77–95.

Turpeinen, O. M., T. L. Garand, R. Benoit, and M. Roach, 1990: Diabatic initialization of the Canadian regional finite-element (RFE) model using satellite data. Part I: Methodology and application to a winter storm. *Mon. Wea. Rev.*, **116**, 2593–2613.

Wang, W., and T. T. Warner, 1988: Use of four-dimensional data assimilation by Newtonian relaxation and latent-heat forcing to improve a mesoscale-model precipitation forecast: A case study. *Mon. Wea. Rev.*, **116**, 2593–2613.

Willoughby, H. E., 1979: Excitation of spiral bands in hurricanes by interaction between the symmetric mean vortex and a shearing environment steering current. *J. Atmos. Sci.*, **36**, 1226–1238.

——, 1990: Gradient balance in tropical cyclones. *J. Atmos. Sci.*, **47**, 265–274.

Yanai, M., S. Esbense, and J.-H. Chu, 1973: Determination of bulk properties of tropical cloud clusters from large-scale heat and moisture budgets. *J. Atmos. Sci.*, **30**, 611–627.

Zhang, G. J., and H.-R. Cho, 1991: Parameterization of the vertical transport of momentum by cumulus clouds. Part I: Theory. *J. Atmos. Sci.*, **48**, 1483–1492.